

APPLICATION OF HEATING MICROSCOPY ON SINTERING AND MELTING BEHAVIOUR OF NATURAL SANDS OF ARCHAEOLOGICAL INTEREST

FRANCESCO MONTANARI*, CRISTINA BOSCHETTI**, PAOLA MISELLI*, MIRIAM HANUSKOVA*, PIETRO BARALDI***, CRISTINA LEONELLI*

*Department of Engineering "Enzo Ferrari", University of Modena and Reggio Emilia,
Via Vignolese 905, 41125 Modena, Italy

**Department of Archaeology, University of Nottingham, NG7 2RD Nottingham, UK

***Department of Chemical and Geological Sciences, University of Modena and Reggio Emilia,
Via Campi 183, 41125 Modena, Italy

#E-mail: cristina.leonelli@unimore.it

Submitted March 6, 2013; accepted September 30, 2013

Keywords: Hot stage microscope, Sintering curves, Natural sand, Meltability, Ancient vitreous materials

In antiquity, beach sand was one of the main raw materials for glass-making and for the production of other vitreous materials, like Egyptian blue and faience. During the 1st century AD, glass and pigments manufacturing industry was active along the Gulf of Naples, Italy, where we sampled four littoral sands. Samples were analyzed with different techniques: chemical analysis was performed by means of X-Ray Fluorescence (XRF) and mineralogical analyses with X-Ray Powder Diffraction (XRPD) and Raman Spectroscopy. The complete sintering to melting thermal behaviour of the four sands was studied by heating microscopy or hot-stage microscope (HSM) equipped with an high resolution camera capable to collect sample profile during heating. The effect of the grain size on the sintering curves, which were automatically elaborated by specimen profile transformation, was also investigated. Finally, some deductions about the granulometry effect and the presence of alkaline and alkaline-earth oxides on sintering and melting behaviour were drawn. All the four sands were found suitable for highly sintered manufactures rather than glasses, to reach complete amorphous materials the addition of fluxes was necessary.

INTRODUCTION

Silica, together with a flux and calcium carbonate, is one of the most important components to produce soda lime glass [1]. Naturally combined with calcite and low amounts of sodium feldspar, beach sand was used since the origin of glass and vitreous materials industry. The batch was prepared by mixing sand with a flux, natron or plant ashes, and the final product was obtained in a single or two stage melting [2]. The product of this process was the raw glass, characterised by a greenish or yellowish colour due to the natural impurities contained in the raw materials [3]. The Latin author Pliny the Elder describes, in the middle 1st century AD, the presence of a glass-making activity also in the Gulf of Naples, between the towns of Cuma and Liternum, in his *Naturalis Historia* (36, 194) [4]. In detail, Pliny refers that the softest and whitest part of the sand from a beach near the River Volturno, was ground and used to make glass. This passage is widely discussed, because the actual presence of a glass-making activity in the area has never been documented archaeologically. The suitability for glass-making of sands sampled along the Campanian coast was

tested in literature over the last years with different results [5-7] with the conclusion that a combination of crushing, grinding and washing resulted in an overall composition suitable for glass melting. Additional information on the suitability of sands for glass-making in Italian area at Romans time comes from compared studies on chemical composition [8]. The results indicated that few of the 178 analysed beach sands have been suitable to produce a glass with major and minor elemental compositions within the ranges of Roman imperial natron glass. In particular, the sands sampled in the Naples Gulf are too rich in CaO to match the required compositions.

If the results seem to reject the hypothesis that glass was made with sands from the Gulf of Naples, the archaeological evidence of a production of Egyptian blue pigment in this area needs to be mentioned. Here, in the sites of Cumae and Liternum, different excavation contexts have systematically revealed fragments of cylindrical crucibles, with remains of the material adhered on the walls [9]. Egyptian blue is a partially vitrified material mainly composed of cuprarivaite and silica polymorphs, embedded in a glass matrix [10]. A production in the Hellenistic period is documented in Egypt, at Memphis,

but analysis conducted on Roman samples from Greece, Italy and Egypt have revealed differences in the chemical composition, suggesting the existence of more than one productive centre [11]. Presently, the crucibles from the Gulf of Naples are the only indicators of Egyptian blue production documented in the Western Mediterranean.

Moreover, we need to consider a possible relation with faience, another sintered material produced by the ancient industry and characterized by different technological variants, i.e. with or without a surface glazing [12]. A recent investigation on faience vessels and statuettes from Pompeii has suggested the existence of a possible local production, specialized in the imitation Egyptian materials. The samples, identified as made locally, are characterized by an anomalous high content in calcium and alumina [13].

The present paper wants to be a complete study on four sands, collect around Naples, in terms of sinterability and meltability to help archaeologists to introduce a discussion on their possible use for the ancient production of partially vitrified materials. The technique used for the melting behaviour is the heating microscope often successfully applied to analyze raw ceramic materials and their properties [14-16]. Such a technique appears particularly attractive for archaeometric investigations since its could be qualified as semi-destructive analyses using only 5 mg of finely crushed sample. Additionally with one heating ramp it is possible to determine the incipient sintering, amorphous phase formation, eventual gas evolution and the interval of melting [17].

EXPERIMENTAL

Four sands were sampled along the Campanian coast where primary production of glass is quoted by the ancient sources [4] and in those locations where evidence for making Egyptian blue is documented [9]. More precisely, the four specimens come from Miliscola, Lido di Licola (near Cuma), Ischitella and Castel Volturno (Neaples, Italy) and were named, respectively, S1, S2, S3 and S4 (Figure 1). Sampling was performed collecting about 4 kg of sand at a depth of about 15 centimetres. The sand was gently blended manually to obtain a good homogeneity, than it was divided 4 part and one sample of 10 g was taken from each part; these 4 samples were again blended and dried in a stove at 120°C.

To evaluate the average chemical composition of the four samples, an X-Ray Fluorescence sequential spectrometer (XRF ARL Advant'XP+, Thermo Fisher Scientific, Waltham, MA, USA) was used. The percentage Loss of Ignition (LoI) was also determined heating the samples to 1150°C. The mineralogical analysis of the sands was carried out by means of X-Rays Powder Diffraction (XRPD, PW-3710, Philips, The Netherlands) with a monochromatic Cu-K α radiation ($\lambda = 1.54060 \text{ \AA}$) and Raman Spectroscopy (LabRAM, Jobin Yvon Inc.,

Longjumeau, France) equipped with He-Ne laser with wavelength = 632.8 nm, spatial resolution = 1 μm , spectral resolution = 1 cm^{-1} , maximum power = 5 mW. The background of the obtained spectra was corrected (shifted and linearized) by using a commercial software (GRAMS/AI 8.0 Thermo Fisher Scientific, Waltham, MA, USA).

The sintering and melting behaviour of the sands was studied with a heating microscope (HSM, Expert System Solutions, Modena, Italy). The relation between the sintering behaviour and the grain size of the samples was also investigated, considering that manual grinding in glass and pigment preparation was a procedure possibly practiced in the ancient industry. Two distinct granulometries were chosen, the coarse (hereafter indicated as C) and the fine (hereafter indicated as F), and grain size distribution was analyzed by a laser light scattering particle size analyzer (MasterSizer 2000 Particle Size Analyzer, Malvern), equipped with a wet state sampler (HYDRO2000S, Malvern). Finally, each of the eight powders was shaped in small cylinders with a height of 3 mm and a diameter of 2 mm and put over alumina slabs inside a small furnace and tested separately with the heating microscope (Misura 3, Expert System Solutions, Modena, Italy). The software supplied with the instrument provides sintering or dilatometric curves from which five temperatures can be derived, namely: (I) the first shrinkage or sintering, (II) the maximum shrinkage before softening starts, (III) the softening point, at which the first signal of melting appears, (IV) the half ball point, when the specimen forms a semicircle, and (V) the flow point, at which the test piece collapses to a third of its height at the hemisphere state (following standards ISO 540 1995-03-15/DIN 51730 1998-04 [18-19]). Some of these temperatures were defined by

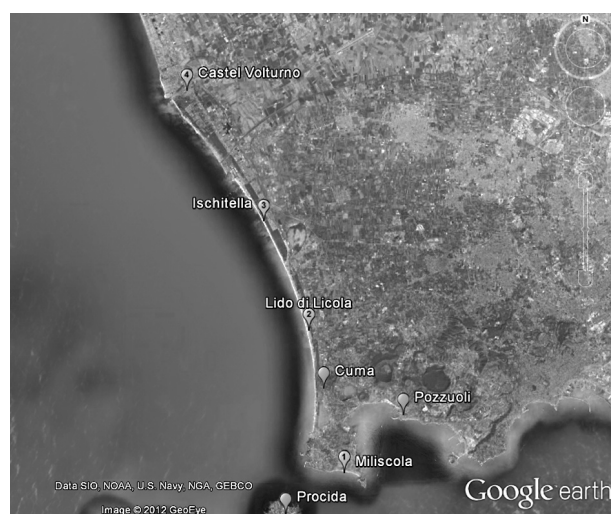


Figure 1. A satellite image of the Campanian littoral (Italy). The picture was taken from Google Earth and downloaded on March 2nd, 2012 (<http://earth.google.com/>). The places where the sands (S1, S2, S3 and S4) were sampled are marked with their relative numbers.

Scholze in 1962 [20] and each one corresponds to a characteristic viscosity point, conventionally determined on the basis of geometrical considerations.

RESULTS AND DISCUSSION

The as-received sands were melted in sodium borate pearl to attain the necessary homogeneity for X-ray fluorescence analysis. Table 1 shows the XRF chemical compositions and the main crystalline phases. Traces of heavy metals, chlorine and bromine, below 0.1 % were also found. As a general observation, we can observe that the amount of SiO₂ is compatible with the content in silica for Roman glasses, but the presence of Al₂O₃ and iron oxides seems to confirm the recent observation by Brems and co-authors [8], also advanced in previous investigations [21-23], which found rocks contamination deriving from mafic volcanic activity on the littoral sands.

Table 1. XRF Chemical compositions (oxides in % weight and normalized to 100 %) of the four sands, together with their LoIs and crystalline phases from XRD analyses.

Oxides	S1	S2	S3	S4
SiO ₂	50.30	47.00	60.70	53.60
Al ₂ O ₃	14.80	7.84	8.16	6.79
CaO	8.29	20.70	11.30	17.30
MgO	1.75	0.93	1.17	2.88
Na ₂ O	3.29	1.70	4.50	2.54
K ₂ O	5.70	3.28	3.45	2.54
Fe ₂ O ₃	4.64	1.73	1.87	3.38
TiO ₂	0.51	0.16	0.17	0.35
LoI	10.10	15.90	7.90	9.30
SiO ₂ /CaO	6.06	2.34	5.37	3.09
Quartz (SiO ₂)	xxxx	xxxx	xxxx	xxxx
Calcite (CaCO ₃)	xx	xxx	xxx	xxx
(Ca/K/Na)-feldspar	xxx	xx	xxx	xx
Clay minerals	x	x	x	x

The presence of alumina increases the refractoriness of the sands and make them more suitable for the production of sintered materials rather than for glass-melting. As described by Silvestri and co-authors [5], in order to produce effectively a colourless glass, a long procedure of grinding, washing and sieving would have been necessary, to eliminate the feldspatic phases, responsible of introducing Al₂O₃. Roman glasses show a typical CaO content of 5 - 10 % [3] and, considering the thermal treatment, the calcium content in the sands is estimated to be around 6 - 11 % [6]. Considering these parameters, we can observe that three of the sands analysed (S2, S3, S4) have a content in CaO between the 8.29 and the 20.7 %, sensibly higher if compared to the amount detectable in Roman glasses. However, this

content in CaO is compatible with the amounts observed in Ptolemaic and Roman samples of Egyptian blue, where the content in CaO (bulk composition) ranges from 7.4 to 17.4 % [11]. Similarly, a high content in CaO (17.62 - 19.86 %) was detected in the body of two faïences from Pompeii, interpreted as a Roman imitation of Egyptian productions [13].

Considering the SiO₂ and the fluxes content, the classification of the refractoriness of the sands should be S3, S4, S1 and S2. Furthermore, high percentages of Fe₂O₃ characterise the specimens S1 and S4; its presence actually modifies the colour of a typical soda-lime glass, leading to a blue-greenish hue [2]. The LoI of a natural sand is usually associated to the presence hydroxides and organic materials (including pulverised seashells), jointly with the presence of mineral carbonates. The sands S2, S1, S4 and S3, in the order, exhibit a decreasing value of LoI, indicating a decreasing presence of calcium oxide in a carbonatic phase. No trace of aragonite, a polymorph form of CaCO₃, typical of seashell, was found in the 4 sands as well as crystalline phases of chlorides and bromides indicating a good level of purity of the sands as raw materials.

Raman microscopy (Figure 2) revealed the presence within the sands of traces of various minor crystalline phases, in addition to all those already detected by means of XRPD. In the sand S1 we found a crystal of analcime (NaAlSi₂O₆·H₂O) (Figure 2a), an area constituted by phillipsite-Ca (Ca₃(Si₁₀Al₆)O₃₂·12H₂O) and diopside (CaMgSi₂O₆) (Figure 2b) and a zone with hematite (Fe₂O₃), magnetite (Fe₃O₄) and diopside (Figure 2c) [24]. A crystal of nepheline (KNa₃(AlSi₄)₄) was detected within the sand S2 (Figure 2d) [24]. XRD and RAMAN data well fit with mineralogical characterization from reference [25] of fairly pure sands with calcite and minor quantities of feldspar.

Grain size distribution curves (Figure 3) are all bimodal and almost coincident for both kind of specimens, namely C and F powders, indicating the presence of two families of mineral with different hardness, hypothetically being quartz the harder one in respect to the others, such as calcium carbonate or feldspars. The fineness of the powders is expected to have the same effect on each sample, despite their different chemical compositions as evidenced in the sintering curves (Figure 4). For an easier comparison, the two plots, one for each grinding procedure, C and F, were superimposed for each sample. Additionally, Table 2 shows the five characteristic temperatures of the four sands calculated by the software Misura 3 or identified manually. As a matter of fact as all the samples were crystalline materials, the sphere and the half sphere geometries were generated with an irregular shape differently from glass specimen and were not detected automatically by the software. Nevertheless, the free-sintering curves are helpful to follow sintering phenomena in terms of densification and expansion of multicomponent mixtures [26], such as the four studied

Table 2. Characteristic temperatures (sintering, softening, sphere, half sphere and flow) provided by the heating microscope software Misura 3 for the four sands, ground both coarsely C and fine F.

	S1-C	S1-F	S2-C	S2-F	S3-C	S3-F	S4-C	S4-F
T _{sintering} (°C)	1150	1111	1179	1187	1180	1162	1211	1170
T _{softening} (°C)	1221	1116	1290	1276	1280	1253	1260	1220
T _{sphere} (°C)	–	1200	–	–	–	1271	–	1255
T _{half sphere} (°C)	1247	1228	1312	1295	1327	1283	1267	–
T _{flow} (°C)	1262	1253	1317	1301	1342	1317	1273	1258

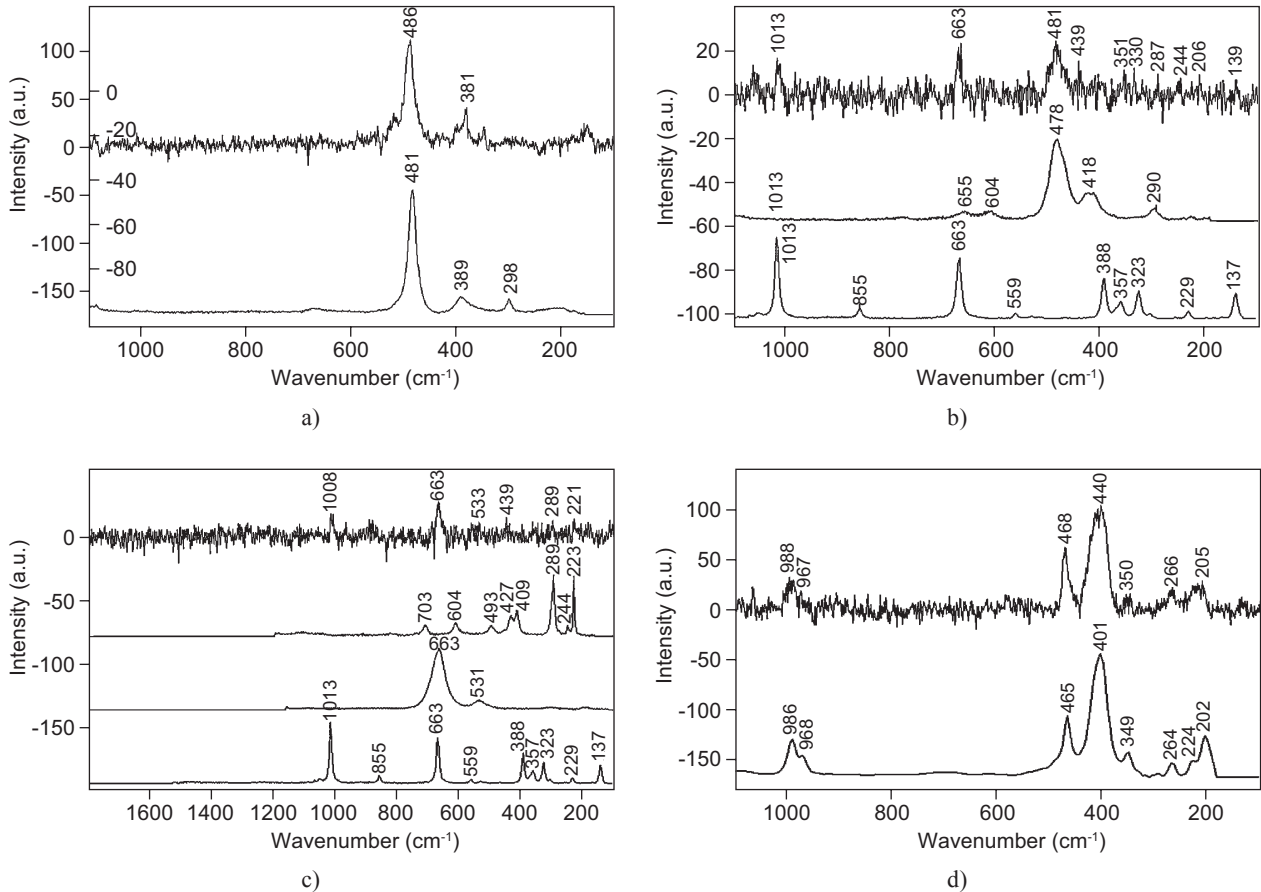


Figure 2. Raman spectra (in top) of: a crystal of analcime (its reference below) (a), an area constituted by phillipsite-Ca (its reference in the middle) and diopside (its reference below) (b), a zone made up of hematite (its reference up), magnetite (its reference in the middle) and diopside (its reference below) (c) in the sand S1 and a crystal of nepheline (its reference below) (d) in the sand S2.

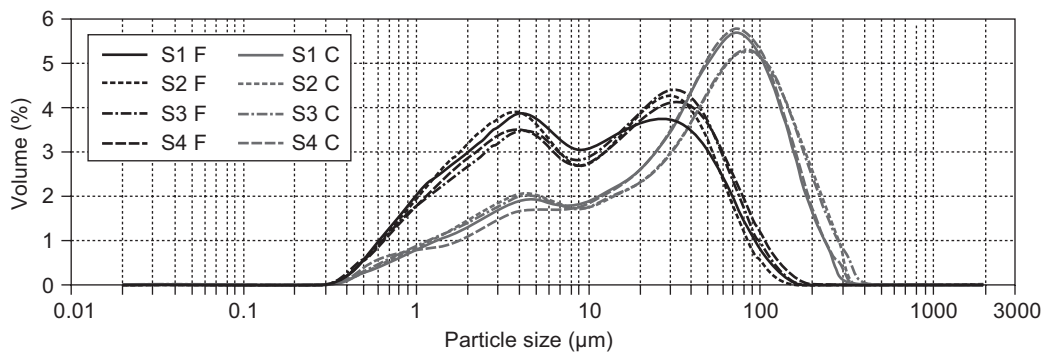


Figure 3. Laser particle size analysis distribution curves of the four sands, S1, S2, S3 and S4, ground both coarsely C and fine F.

sands. Each plot is characterised by a long plateau (characterised by a small contraction (about 2.5 %) around the range 800 - 850°C up to the melting point in a range between 1100 and 1150°C, independently by the finesse of grinding. The contraction at about 800°C may have been caused by the presence of organic substances burnt out during the heating cycle or by the decarbonation of some minerals, such as calcite. Finally, the melting process starts at the end of each plateau with a sudden drop of the sintering percentage, completely vertical for the specimens S2 and S4. Moreover, this process is completed in a very narrow temperature range as typical of the formation of a liquid phase possibly associated to a ternary or quaternary eutectic compound. After this shrinkage, a very short plateau may indicate the formation of a crystalline phase that inhibited the densification process. Furthermore, in the cases of the sands S1 and S2, the curves show a little expansion respectively around 1160 and 1260°C during the melting process, probably due to the increase of volume of some minerals, the formation of new phases or the formation of a gas phase in presence of a liquid. The literature reports a similar phenomenon in the same temperature range [27], where the deformation is accompanied by a volume increase due to the reduction of Fe^{+3} to Fe^{+2} and gas release.

At higher temperatures up to the melting point, all the sintering curves of Figure 4 show the collapse of the cylindrical sample, indicating a high amount of liquid phase. In detail, the melting temperature, where each plot ends, does not seem to depend on the grain size of the powdered specimen and indicate the less melttable sand being S3, followed by the specimens S2, S4 and S1 in the order. In general, finer is the grinding, lower are the characteristic temperatures obtained by the HSM, indicating that the specific surface area is the driving force of the sintering and/or melting phenomena.

The presence of the first drop of liquid during heating and hence the meltability of the four samples as obtained by the sintering curves of the heating microscope can be explained using the ternary phase diagram SiO_2-Na_2O-CaO [28] (Figure 5), using the chemical compositions of the four sands (Table 1) and rescaling to 100 % the percentages of the three main oxides (K_2O , Al_2O_3 , and Fe_2O_3 excluded). Figure 5 shows that the sample S3 is again the most refractory, followed by S2 and, even if with little differences (about 50°C lower), by S1 and S4. Finally, although the results provided by the heating microscope showed that the sands S1 and S4 have very close flow points, the ternary phase diagram SiO_2-Na_2O-CaO highlights that S1 is less melttable than S4. The presence of a high content of potassium oxide,

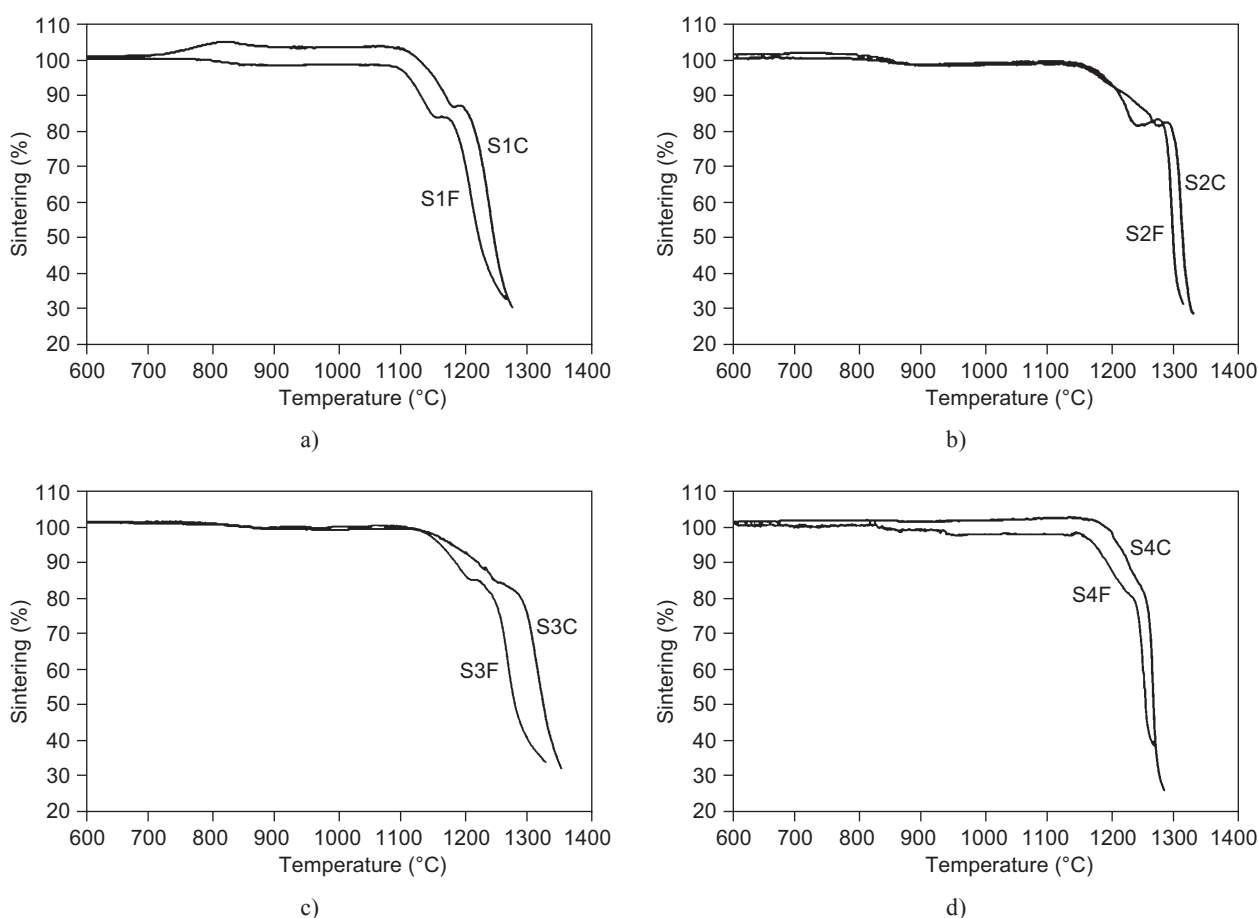


Figure 4. Sintering curves (Sintering % vs T) of the four sands S1 (a), S2 (b), S3 (c) and S4 (d), ground both coarsely C and fine F.

which was not previously taken into account in the interpretation based on ternary phase diagram of Figure 5, could be an additional explanation for the high meltability of the sample S1. We also analyzed the presence of Al_2O_3 , observing that its amount is strictly related to the content of Na_2O and K_2O (Table 1). Therefore, we can conclude that the alkaline cations are present mainly in the feldspatic mineral components, making the sample S1 the easiest to melt among the examined natural sands.

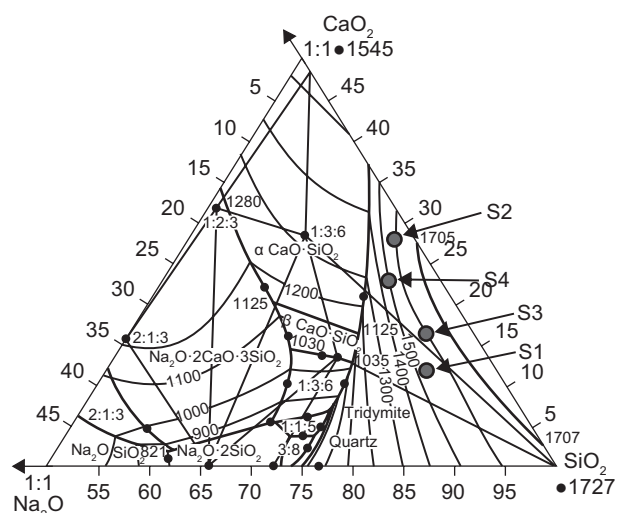


Figure 5. Ternary phase diagram SiO_2 - Na_2O - CaO (taken from Ref. [27], modified). The compositions of the four sands S1, S2, S3 and S4 are indicated.

CONCLUSIONS

This study has demonstrated that the heating microscope is a very versatile and powerful instrument to characterise ceramic raw materials. The temperatures provided by this instrument show a slight dependency on the grain size of the powdered samples. In detail, finer is the grinding of the specimens, lower are the characteristic temperatures provided by the software supplied with the heating microscope. This behaviour is caused by the increase of the average specific surface area. Additionally, various phenomena related to the specific surface area, such as superficial crystallization or gas evolution, become more evident in finer powders.

The chemical, mineralogical and thermal analyses showed that the four natural sands, sampled along the Campanian coast (Italy), are characterised by a thermal behaviour compatible with the temperatures reachable by the ancient vitreous materials technology, below the 1200°C [28-30]. In particular, their flow points fit well with the melting temperatures commonly observed in natural sands with high silica contents [31]. However, considering the high content in calcium, these sands

can be considered an unsuitable raw material for the production of glass, while could have been used in Roman times to manufacture sintered materials, like Egyptian blue and faience.

Finally, all the analyses highlighted that the sand S3 is the most refractory among those studied. According to the literature on the experimental reproduction of Egyptian blue, the temperature estimated for its manufacture is in the range of $900 - 1000^\circ\text{C}$ [10]. Thus, the addition of a flux, for example natron [32], would have been essential to use this sand in a furnace to obtain the synthesis of the pigment.

Acknowledgements

Authors thank Dr. Maria Cannio (University of Modena and R.E.) for her help with the chemical analyses, Prof. Michelina Catauro and Eng. Romolo Laperuta, (Second University of Naples), who helped with the sampling of the sands and finally, the British Academy (Small Research Grant, Albert Reckitt Archaeology Found 2010, project "The provenance of Roman mosaic glass tesserae from Italy", principal investigator Dr. Cristina Boschetti, co-investigator Prof. Julian Henderson) is gratefully acknowledged for the financial support to perform the sampling of the sands.

REFERENCES

1. Pfaender H.G.: *Schott Guide to Glass*, Chapman and Hall, London 1996.
2. Sayre E.V., Smith R. W.: *Science* 133, 1824 (1961).
3. Jackson, C.M.: *Archaeometry* 47, 763 (2005).
4. Eichholz D.E.: *Pliny – Natural History*, vol. X, book XXXVI, Heinemann, London/Harvard, University Press, Cambridge (MA, USA) 1962.
5. Silvestri A., Molin G., Salviulo G., Schievenin R.: *Archaeometry* 48, 415 (2006).
6. Brems D., Ganio M., Latruwe K., Balcaen L., Carremans M., Gimeno D., Silvestri A., Vanhaecke F., Muechez P., Degryse P.: *Archaeometry* 55, 214 (2013).
7. Brems D., Ganio M., Latruwe K., Balcaen L., Carremans M., Gimeno D., Silvestri A., Vanhaecke F., Muechez P., Degryse P.: *Archaeometry* 55, 449 (2013).
8. Brems D., Degryse P., Hasendoncks F., Gimeno D., Silvestri A., Vassilieva E., Luypaers S., Honings J.: *J. Archaeol. Sci.* 39, 2897 (2012).
9. Caputo P., Cavassa L. in: *Artisanats antiques d'Italie et de Gaule: Mélanges offerts à Maria Francesca Buonaiuto, Collection du Centre Jean Bérard 32. Archéologie de l'artisanat antique 2*, p. 169-179, Ed. Brun J.-P., Naples: Centre Jean Bérard, Naples 2009.
10. Hatton G.D., Shortland A.J., Tite M.S.: *J. Archaeol. Sci.* 35, 1591 (2008).
11. Tite M.S., Hatton G.D. in: *Communities and Connections: Essays in Honour of Barry Cunliffe*, p. 75-92, Ed. Gosden C., Hamerow H., de Jersey P., Lock G., Oxford University Press, Oxford (MS, USA) 2007.

12. Tite M.S., Bimson M.: *Archaeometry* 28, 69 (1986).
 13. Mangone A., De Benedetto G.E, Fico D., Giannossa L.C., Laviano R., Sabbatini L., van der Werf I.D., Traini A.: *New J. Chem.* 35, 2860 (2011).
 14. Paganelli M., Sighinolfi D.: *Ceram. Forum Int.* 85, E63 (2008).
 15. Kronberg T., Fröberg K.: *Ceram. Eng. Proc.* 22, 167 (2001).
 16. Dondi M., Guarini G., Venturi I.: *Ind. Ceram.* 21, 67 (2001).
 17. Montanari F., Miselli P., Boschetti C., Baraldi P., Henderson J., Leonelli C.: *Int. J. Appl. Glass Sci.*, in press (2013).
 18. DIN 51730 (1998-04): *Determination of fusibility of fuel ash.*
 19. ISO 540-1995 (1995-03-15) *Solid mineral fuels - determination of fusibility of ash - high-temperature tube.*
 20. Scholze H.: *Ber. Dtsch. Keram. Ges.* 39, 63 (1962).
 21. Brill R.H.: *Chemical Analyses of Early Glass*, Vol. 1 and 2, The Corning Museum of Glass, Corning (NY, USA) 1999.
 22. Turner W.E.S.: *J. Soc. Glass Technol.* 40, 277 (1956).
 23. Vallotto M., Verità M. in: *Homo Faber: Studies on Nature, Technology and Science at the Time of Pompeii*, p. 63-67, Ed. Castagnetti G., Renn J., "L'erma" di Bretschneider, Rome 2002.
 24. <http://rruff.info>.
 25. Verità M. in: *Vitrum: il vetro tra arte e scienza nel mondo romano*, p. 163-167, Ed. Beretta M., Di Pasquale G., Firenze Musei, Giunti Editore, Florence/Milan 2007.
 26. Ergul S., Ferrante F., Piscicella P., Karamanov A., Pelino M.: *Ceram. Int.* 35, 2789 (2009).
 27. Levin E.M., Robbins C.R., McMurdie H.F., Reser M.K.: *Phase diagrams for Ceramists*, American Ceramic Society, Columbus (OH, USA) 1964.
 28. Bingham P.A., Jackson C.M.: *J. Archaeol. Sci.* 35, 302 (2008).
 29. Taylor M., Hill D.: *J. Glass Stud.* 40, 249 (2008).
 30. Lahlil S., Biron I., Cotte M., Susini J.: *Appl. Phys. A: Mater. Sci. Process.* 100, 683 (2010).
 31. Ademoh N.A.: *Am.-Eurasian J. Sci. Res.* 3, 75 (2008).
 32. Shortland A.J., Degryse P., Walton M., Geer M., Lauwers V., Salou L.: *Archaeometry* 53, 916 (2011).
-